Chemistry–A European Journal
Research Article
doi.org/10.1002/chem.202403002
Chemistry Europe
European Chemical Societies Publishing
www.chemeurj.org

Hot Paper

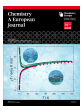

Dinuclear Dysprosium Compounds: The Importance of Rigid Bridges

Rouven F. Pfleger,[a] Matteo Briganti,[e] Niels Bonde,[d] Jacques Ollivier,[f] Jonas Braun,[a, b, c] Thomas Bergfeldt,[g] Stergios Piligkos,[d] Thomas Ruppert,[a] Christopher E. Anson,[a] Mauro Perfetti,*[e] Jesper Bendix,*[d] and Annie K. Powell*[a, b, c]

We report the synthesis, structures and magnetic behaviour of two isostructural dinuclear Dy^{3+} complexes where the metal ions of a previously reported monomeric building block are connected by a peroxide (O_2^{2-}) or a pair of fluoride ($2\times F^-$) bridges. The nature of the bridge determines the distance between the metal ion dipoles leading to a dipolar coupling in the peroxido bridged compound of only ca. 70% of that in the *bis*-fluorido bridged dimer. The sign of the overall coupling between the metals is antiferromagnetic for the peroxido bridged compound and ferromagnetic for the *bis*-fluorido bridged complex. This in turn influences the magnetisation dynamics. We compare the relaxation characteristics of the dimers with those of the previously reported monomeric building block. The relaxation dynamics for the *bis*-fluorido system are very fast. On the other hand, comparing the properties of the monomer, the peroxido bridged sample and the corresponding Y-doped sample show that the relaxation properties via a Raman process have very similar parameters. We show that a second dysprosium is important for either tuning or detuning the Single Molecule Magnet (SMM) properties of a system.

Introduction

Research into lanthanide Single Molecule Magnets (SMMs) has led to significant improvements in terms of slow relaxation of the magnetisation since these properties were discovered in this class of compounds.[1–3] Design principles for single ion lanthanide SMMs and in particular those containing dysprosium or erbium in the trivalent oxidation state still require further development in order to achieve high performance systems.[4–17]

One of the open challenges in the field is to understand and control the relaxation pathways for the magnetization. Indeed, undesirable relaxation mechanisms such as Raman or Quantum Tunnelling of the Magnetisation (QTM) can decrease the relaxation time by several orders of magnitude compared to the classical thermally activated Orbach process.[18,19] Chemical tools for circumventing QTM have been described.[20] Appropriate coordination geometries reduce the mixing of states therefore hampering the quantum tunnelling events.[21–24] Weak transversal magnetic fields, that facilitate forbidden transitions, can in some cases be significantly reduced by using isotopically pure samples eliminating the influence of hyperfine coupling to the nuclear spin.[25,26] Furthermore, diluting the magnetic complexes in isostructural diamagnetic hosts to quench weak magnetic interactions between neighbouring magnetic centres can quench undesired under-barrier relaxation pathways.[27–31] Raman relaxation is more challenging to control. Some progress in understanding the connection between Raman relaxation and the nature of phonons involved in these processes has been achieved, but there is still an open debate about the best way to treat these contributions.[32–38]

In the case where nuclearity is increased to two dysprosium ions comparisons of the bulk systems with magnetically diluted systems reveal that the SMM performance can be both improved (tuned) or made worse (detuned) although the reasons for this are far from clear.[39–42]

Something lacking in this field is the availability of studies where a characterised mononuclear building block is linked using different bridges. This would allow correlations to be

[a] R. F. Pfleger, J. Braun, T. Ruppert, C. E. Anson, A. K. Powell
Institute of Inorganic Chemistry, Karlsruhe Institute of Technology (KIT), Kaiserstr. 12, 76131 Karlsruhe, Germany
E-mail: annie.powell@kit.edu
[b] J. Braun, A. K. Powell
Institute of Nanotechnology, Karlsruhe Institute of Technology (KIT), Kaiserstr. 12, 76131 Karlsruhe, Germany
E-mail: annie.powell@kit.edu
[c] J. Braun, A. K. Powell
Institute for Quantum Materials and Technologies, Karlsruhe Institute of Technology (KIT), Kaiserstr. 12, 76131 Karlsruhe, Germany
E-mail: annie.powell@kit.edu
[d] N. Bonde, S. Piligkos, J. Bendix
Department of Chemistry, University of Copenhagen, Universitetparken 5, 2100 Copenhagen, Denmark
E-mail: bendix@chem.ku.dk
[e] M. Briganti, M. Perfetti
Department of Chemistry "U.Schiff", University of Florence, Via della Lastruccia 3–13, Sesto Fiorentino, Italy
E-mail: mauro.perfetti@unifi.it
[f] J. Ollivier
Institut Laue-Langevin, 71 avenue des Martyrs, CS 20156, 38042 Grenoble Cedex 9, France
[g] T. Bergfeldt
Institute for Applied Materials, Karlsruhe Institute of Technology (KIT), Kaiserstr. 12, 76131 Karlsruhe, Germany

made regarding the influence of the nature of the bridging units between dysprosium ions on the magnetic properties. Here we present for the first time such a system where two mononuclear $[Dy(H_2dapp)(NO_3)_2](NO_3)$[43] building blocks are linked with either fluorido or peroxido bridges. Another strategy is to use bridging species such as inverse hydrogen bonding to link the building blocks.[44,45]

Fluoride and peroxide ligands are not commonly used species in the synthesis of lanthanide complexes since these hard anions often lead to the formation of stable lanthanide salts, explaining the meagre number of publications on lanthanide complexes with fluoride[46–55] and peroxide[56–67] ligands with only one example where H_2O_2 was purposely added.[68] In this paper we describe suitable reaction conditions that make these coordination compounds readily accessible and investigate their magnetic behaviour.

Results and Discussion

2,6-*bis*((*E*)-1-(2-(pyridin-2-yl)-hydrazineylidene)ethyl)pyridine (H_2dapp) has hardly been used in coordination chemistry.[69–71] We have previously shown that monomeric $[Dy(H_2dapp)(NO_3)_2]^+$ complexes show field induced SMM behaviour which is dependent on the counterion.[43]

The H_2dapp Schiff base ligand is formed *in situ* (Scheme 1). Stirring a methanolic solution of two equivalents of 2-hydrazinopyridine and one equivalent of 2,6-diacetylepyridine with one equivalent of $Dy(NO_3)_3 \cdot 6H_2O$ and subsequent heating gives the monomeric complex $[Dy(H_2dapp)(NO_3)_2](NO_3)$ (hereafter[18]) which crystallises immediately upon cooling.

Using the same reaction procedure as for the mononuclear system,[18] but without any heating, prevents the crystallisation of[18] from solution. Upon addition of 1.2 equivalents of H_2O_2 followed by the addition of one equivalent of Et_3N the peroxido bridged $[Dy_2(\mu\text{-}O_2)(H_2dapp)_2(NO_3)_2](NO_3)_2$ (hereafter $\{Dy_2(O_2)\}$ **1**) crystallises.

For the synthesis of $[Dy_2(\mu\text{-}F)_2(H_2dapp)_2(NO_3)_2](NO_3)_2$ (hereafter $\{Dy_2F_2\}$ **2**) no base is added but 1 equivalent of Et_4NF is added instead of H_2O_2.

The compounds $\{Dy_2(O_2)\}$ **1** and $\{Dy_2F_2\}$ **2** crystallise from their respective methanolic mother liquors as isomorphous *bis*-methanol solvates **1a** and **2a** in the triclinic space group $P\bar{1}$ with $Z=1$ (see Figure 1). On exposure to air, these crystals rapidly exchange their lattice methanols for atmospheric water, forming the corresponding tetrahydrates **1b** and **2b**, crystallising in the acentric monoclinic space group $P2_1$ with $Z=2$. Such a topotactic single-crystal to single-crystal (SC-SC) transition from a centrosymmetric triclinic structure to an acentric monoclinic one is perhaps unexpected. However, comparison of the respective unit cells (Table S1) and the packings in the two crystal forms (Figures S1 and S2) show that it can be understood in terms of a transformation of the unit cell of **1a** by the matrix {1 0 0 −1 −1 −2 0 1 0}, which generates a cell with $a=9.89$, $b=22.86$, $c=11.03$ Å, $\alpha=90.8$, $\beta=98.7$, $\gamma=93.5°$. This compares well with that for **1b**, only requiring adjustments of α and γ from 90.8 and 93.5 to 90°. However, comparison of the packing in the two crystal forms (Figure S1 and S2) shows that the dinuclear complexes in every second layer within the

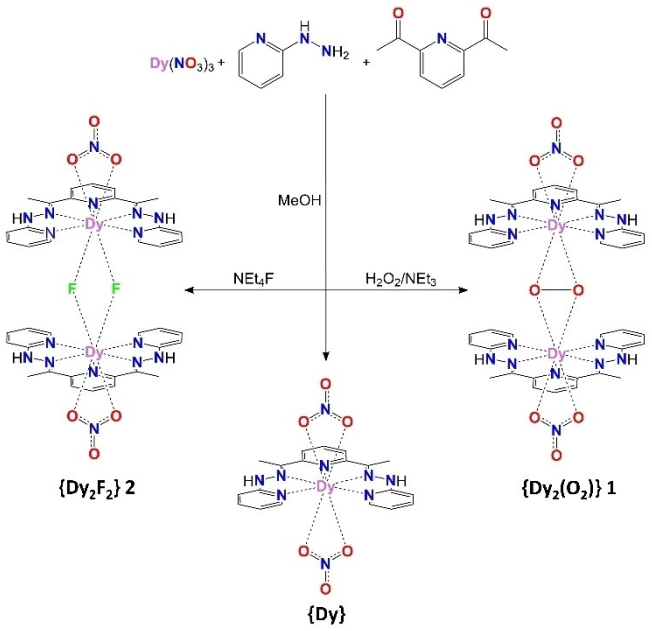

Scheme 1. Synthetic strategy used to obtain $\{Dy_2(O_2)\}$ (right), $\{Dy_2F_2\}$ (left) and {Dy} (bottom).

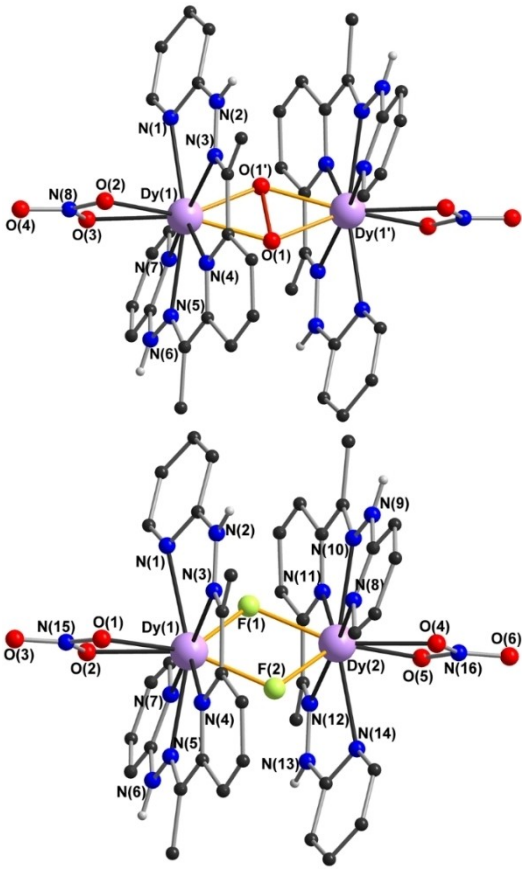

Figure 1. Molecular structures of $\{Dy_2(O_2)\}$ **1** (top) and $\{Dy_2F_2\}$ **2** (bottom).

structure have significantly rotated on going from the triclinic to the monoclinic structure, and the change in lattice solvent has also resulted in a reorientation of the nitrate counteranions. Given the nature of this topotactic transition, it is perhaps surprising that it was in any way possible to determine and refine the structure of the tetrahydrate, however the phase change only seems to manifest itself in the crystal structure by the presence of pairs of "Dy ghost atoms" displaced along the Dy···Dy vector; such "ghosts" are often seen in structures with improperly resolved stacking faults in the crystal.

For the *bis*-fluorido analogue $[Dy_2(\mu\text{-}F)_2(H_2dapp)_2(NO_3)_2](NO_3)_2$ (**2**), this transformation seems even more facile. Although crystals with unit cells corresponding to that of **1a** could be found, the diffraction from these was poor and suggested the phase transition had already begun. For both compounds **1** and **2**, the magnetic measurements were carried out on the respective tetrahydrates as the stable form as shown by PXRD (Figures S3 and S4).

The molecular structures of the peroxido and *bis*-fluorido complexes are shown in Figure 1. Both complexes consist of two Dy ions, each of which is chelated by an H_2dapp ligand and capped by a chelating nitrate; the two Dy are then bridged either by a side-on η^2-peroxide ion or by two fluoride ions. The identity of the fluoride bridges was confirmed by elemental analysis to check that these were not hydroxides.[72,73] Charge balance is provided by two nitrate counteranions.

In both complexes, the Dy–N distances are in the range 2.470–2.540 Å, similar to those reported in the mononuclear $[Dy(H_2dapp)(L)_n]$ {Dy} complexes, with the H_2dapp ligand also showing a similar helical distortion.[43] In **1a**, Dy(1)–O(1) and Dy(1)–O(1′) are 2.2205(18) and 2.2085(18) Å, respectively, in the range expected for lanthanide peroxide bonds,[11] while the peroxide bond length O(1)–O(1′) is 1.544(3) Å and the Dy(1)···Dy(1′) separation is 4.1513(4) Å. The structure of the *bis*-fluorido complex in **2b** differs only in the geometries of the bridging ligands. The Dy–F bond lengths are in the range 2.187(6)–2.260(6) Å, and thus comparable to the Dy-peroxido bond lengths. However, the non-bonding F(1)···F(2) distance, 2.464(7) Å, is now much longer than the peroxide single bond, and this is reflected in a shorter Dy(1)···Dy(2) separation, 3.7085(9) Å (Figure 2). The $Dy(O_2)Dy$ moiety in **1a** is strictly planar in consequence of the inversion site symmetry. However, although this is not required by crystal symmetry, the $Dy(F)_2Dy$ moieties in **2b** does not deviate significantly from planarity. The geometries of the cores in **1a** and **2b** are compared in Figure 2.

In contrast to the Dy_2 complexes **1** and **2**, for the doped analogues $[\{Y/Dy\}_2(\mu\text{-}O_2)(H_2dapp)_2(NO_3)_2](NO_3)_2$ (**3**) and $[\{Y/Dy\}_2(\mu\text{-}F)_2(H_2dapp)_2(NO_3)_2](NO_3)_2$ (**4**), the triclinic *bis*-methanol solvates **3a** and **4a** seem to be the stable forms, as shown by PXRD (Figure S5). The structure of a crystal of **4** could be determined and was found to be the trimethanol solvate of **4**, which crystallised in the monoclinic space group *C*2/*c* with Z = 4 (**4c**). Crystals of **3c** were of poorer quality, precluding full refinement, but had a very similar unit cell to **4c**. Comparison of the unit cells of **4c** and **2b** (Table S1) indicates that the cell of **4c** can be regarded as derived from that of **2b** by the matrix transformation {1 0 1 0 −1 0 1 0 −1}, resulting in a transformed

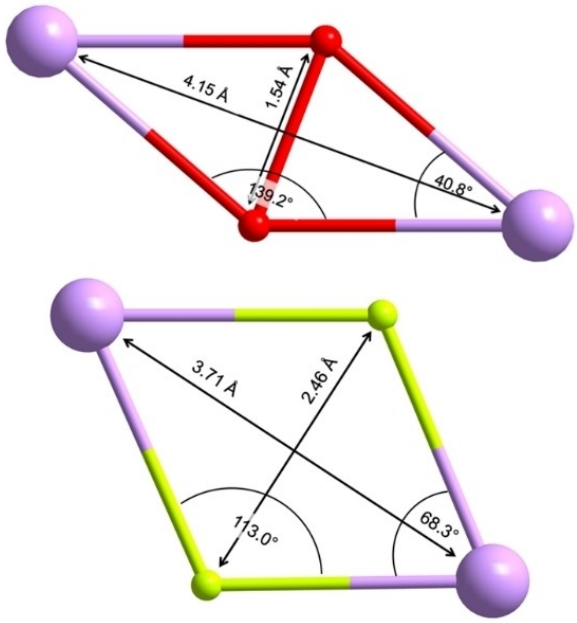

Figure 2. Bond length and angles between the metal centres and the bridging ligands. Colour code: O/red F/green

unit cell with $a = 15.56$, $b = 23.04$, $c = 13.82$ Å, $\alpha = 90$, $\beta = 99.5$, $\gamma = 90°$, which after a *ca.* 15% expansion of the *b*-axis is close to that of **4c**. The metal content in **4c** refined to Y:Dy = 0.949(2):0.051(2). Apart from this, the molecular structure was very similar to that in **2b**, with (Y/Dy)-F distances 2.1949(15) and 2.2137(14) Å and (Y/Dy)1···(Y/Dy)1′ 3.6718(3) Å. However, rather surprisingly no peaks corresponding to this phase could be observed in the PXRD, and it appears that **3c** and 4c both lose two of their four lattice methanols very readily on exposure to air, with phase transitions to **3a** and **4a** (i.e. isomorphous to **1a** and **2a**), respectively (Figure S5).

Crystallographic and refinement parameters are summarised in Table S1, and selected bond lengths and angles are listed in Table S2. Full crystallographic data and details of the structural determinations for the structures in this paper have been deposited with the Cambridge Crystallographic Data Centre as supplementary publication nos. CCDC 2376535–2376537 Copies of the data can be obtained, free of charge, from https://www.ccdc.cam.ac.uk/structures/.

Magnetic measurements on the compounds **1** and **2** were performed on a SQUID magnetometer. As shown in Figure 3, $\{Dy_2F_2\}$ **2** has a χT value of 28.06 $cm^3 mol^{-1} K$ at 270 K (green squares in Figure 3) and $\{Dy_2(O_2)\}$ **1** has a χT value of 27.60 $cm^3 mol^{-1} K$ at 298 K (pink circles in Figure 3), both close to the expected value of 28.34 $cm^3 mol^{-} K$ for two independent Dy^{3+} ions. The χT data of $\{Dy_2(O_2)\}$ **1** show a remarkable decrease below 28 K, reaching 15.35 $cm^3 mol^{-1} K$ at 2 K. This suggests antiferromagnetic coupling as this value is significantly lower than two times the value found for the monomer {Dy}.[43] $\{Dy_2F_2\}$ **2** shows a minimum in the χT versus T graph at 29 K and 25.35 $cm^3 mol^{-1} K$ and a strong increase that leads to the value of 33.89 $cm^3 mol^{-1} K$ at 2 K, implying ferromagnetic coupling

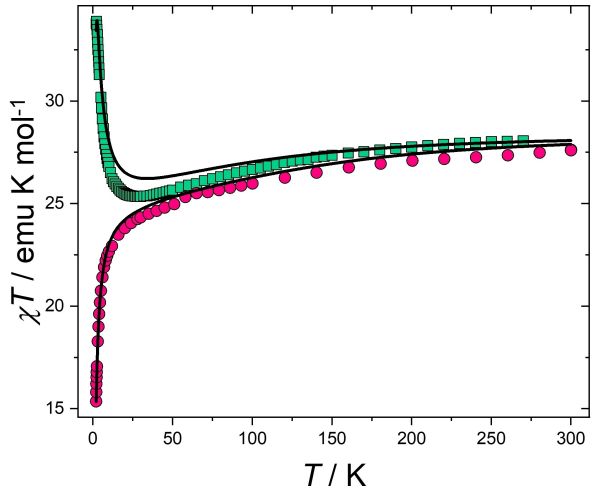

Figure 3. χT vs T plots for $\{Dy_2F_2\}$ (**1 b** green squares) and $\{Dy_2(O_2)\}$ (**2 b** pink circles). The black lines are the best fits (see text).

between the dysprosium centres. The *M* vs *H* plots of both complexes (Figures S7) saturate at 10 μ_B, suggesting strong axiality and a ground doublet with a predominant contribution from the $m_J = \pm 15/2$.

To gain insight into the electronic structure of these complexes we performed multireference *ab initio* calculations using a Complete Active Space Self Consistent Field (CASSCF) approach.[74,75] This enables us to compute the magnetic anisotropy and the energy ladder of single Dy^{3+} ions (see Tables S3 and S4). For both compounds the ground Kramers' doublet shows a magnetic easy axis with g_z values of 19.93 and 19.48 for $\{Dy_2(O_2)\}$ **1** and $\{Dy_2F_2\}$ **2**, respectively. In both cases the axes point along the Dy–Dy direction (see Figure 4). This finding is expected for a Dy^{3+} ion in a low symmetry environment, since the negatively charged ligands dominate and define the electrostatic potential around the lanthanide ion.[76]

Intriguingly, the first excited state of $\{Dy_2(O_2)\}$ **1** is found at 281 cm^{-1} *vs* at 130 cm^{-1} for $\{Dy_2F_2\}$ **2**. Such an energy difference is remarkable and indicates that the peroxide group produces a strong axial crystal field able to stabilise the oblate $m_J = \pm 15/2$ components to a larger extent than is the case for the fluoride ions. Indeed, due to the shorter bonding distance between the oxygen atoms, the ODyO angle is more acute than the FDyF one (see Figure 2) and, as a consequence, the crystal field acting on Dy is more axial in $\{Dy_2(O_2)\}$, leading to a larger CF splitting.

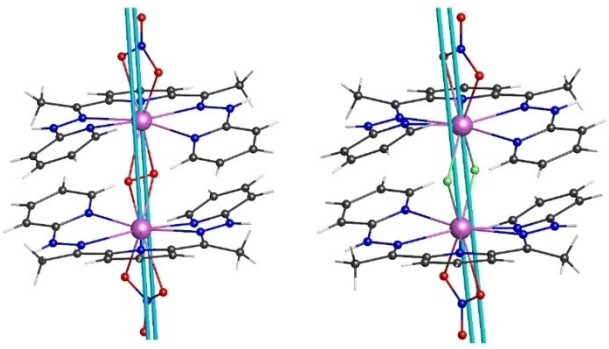

Figure 4. The ground doublet' s magnetic easy axis is shown in light blue. Colour code: Dy/violet, N/blue, F/green, O/red, C/grey, H/white.

In order to help understand the system better inelastic neutron scattering (INS) was performed on $\{Dy_2(O_2)\}$ **1**, and the isostructural analogues $\{Tb_2(O_2)\}$ and $\{Er_2(O_2)\}$ in the energy transfer range 0.2–150 cm^{-1}. For $\{Dy_2(O_2)\}$ **1**, no magnetic excitations were observed which is consistent with our model for which the first excited state is far too high in energy to be sufficiently populated (see Figure S19).

The magnetostructural explanation lies in the difference in the bridging moieties between the Dy^{3+} ions. The marked differences between the magnetic behaviour in both dinuclear compounds can be rationalised as follows. For $\{Dy_2(O_2)\}$ **1** the presence of a short O–O bond has the effect of pushing the Dy^{3+} ions further apart (4.15 Å). However, for $\{Dy_2F_2\}$ **2** since there is no F–F bond the Dy–Dy distance is much shorter at 3.71 Å. For $\{Dy_2(O_2)\}$ **1** the long Dy–Dy distance results in much weaker ferromagnetic dipolar coupling whereas for the $\{Dy_2F_2\}$ **2** the much shorter distance is responsible for stronger ferromagnetic dipolar coupling due to the $1/r^3$ dependency of dipolar coupling. Assuming that the dipoles in both compounds are similar the dipolar coupling in $\{Dy_2(O_2)\}$ **1** will only be 70% of that in $\{Dy_2F_2\}$ **2**. The CF parameters extracted from *ab initio* calculations were used in conjunction with the experimental magnetic data to fit the value of the isotropic coupling constant between the two paramagnetic centres in the dimer. We obtained: $j_{\{Dy2(O2)\}} = +1.03(1)\ \ 10^{-2}\ cm^{-1}$ and $j_{\{Dy2F2\}} = -2.20(1)\ 10^{-2}\ cm^{-1}$ ($+j\ \boldsymbol{J}_1\boldsymbol{J}_2$ convention). The results are shown as black curves in Figure 3. Due to relative orientations of the magnetic easy axes with respect to the Dy–Dy direction (see Figure 1), the dipolar coupling is expected to be ferromagnetic. For the $\{Dy_2F_2\}$ **2** compound this is the dominant interaction pathway. In the $\{Dy_2(O_2)\}$ **1** the dipolar coupling is weaker since the Dy are further apart, the antiferromagnetic nature of the coupling in $\{Dy_2(O_2)\}$ **1** may arise from an antiferromagnetic superexchange interaction mediated by the π-orbitals of the peroxide group which outweighs the weaker dipolar coupling in $\{Dy_2(O_2)\}$ **1**. Such antiferromagnetic coupling was also identified in a peroxido-bridged Cu(II) dimer previously reported which is essentially diamagnetic.[77] Indeed, the ability of p-orbitals on side-on diatomic ligands to mediate antiferromagnetic couplings between lanthanide ions has been demonstrated using DFT calculations.[78,79]

We also performed ac susceptibility measurements to check if the complexes show SMM properties. For $\{Dy_2F_2\}$ **2** an increase of the out-of-phase magnetic susceptibility (χ″) at higher frequencies near the edge of the experimental window suggests a fast relaxation process in the system (Figure S8). This is at odds with the most closely related structure for Dy ions bridged by two fluorides that showed a relaxation time at least two orders of magnitude slower than the one recorded here.[80,81] An explanation for the different behaviour in the present case is related to the contribution to the CF through different ligand sets of the *bis*-fluorido bridged compound we report here to the previously reported one.

$\{Dy_2(O_2)\}$ **1** shows slow relaxation without the need to apply a field (Figure S9). We performed two temperature scans up to 10 K without an applied field as well as in the optimal field of 3000 Oe (Figure 5).

The experimental results, shown as blue squares and red dots in Figure 6, reveal that the application of the external field slows the relaxation rate. The high temperature part of the plot has the same slope for both measurements, suggesting that the thermally activated process is the same.

$$\tau^{-1} = \tau_{tun}^{-1} + B\frac{exp\left(\frac{\hbar\omega}{k_BT}\right)}{\left[exp\left(\frac{\hbar\omega}{k_BT}\right) - 1\right]^2} \quad (1)$$

$$\tau^{-1} = Dcoth\left(\frac{\delta}{k_BT}\right) + B\frac{exp\left(\frac{\hbar\omega}{k_BT}\right)}{\left[exp\left(\frac{\hbar\omega}{k_BT}\right) - 1\right]^2} \quad (2)$$

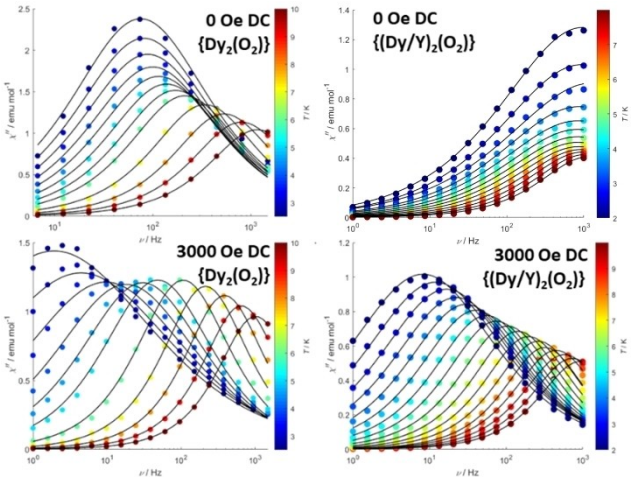

Figure 5. Out-of-phase signals for $\{Dy_2(O_2)\}$ (left) and $\{(Dy/Y)_2(O_2)\}$ (right) in 0 dc field (top) and under 3000 Oe dc field (bottom).

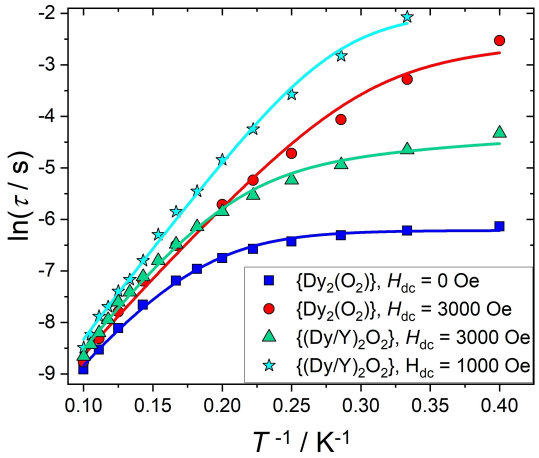

Figure 6. Evolution of the relaxation time of $\{Dy_2(O_2)\}$ (0 Oe, blue squares and 3000 Oe, red diamonds) and $\{(Dy/Y)_2(O_2)\}$ (3000 Oe, green triangles and 1000 Oe, cyan stars). The lines are the best fits (see text).

We fitted the experimental curve in zero field using two terms, according to equation 1. The first term is the quantum tunnelling relaxation rate and the second term is a Raman process where the energy of the involved phonon is $\hbar\omega$. An Orbach process was not included because it did not improve the fit. However, the fitted phonon energy involved in the Raman process (16.5 cm^{-1}) is in line with the energy of phonons calculated for molecular complexes.[37] Indeed, this value is close to those found for {Dy} mononuclear complexes, suggesting that the same vibronic modes could be responsible as found for the relaxation pathway in the mononuclear complex {Dy}.[43]

For fitting the in-field relaxation for an applied field of 3000 Oe we can replace the zero-field quantum tunnelling contribution with a direct process involving a fixed energy gap of $\delta = 2.8\ cm^{-1}$ between the two states of the 15/2 ground doublet along the z axis. This is reasonable because the $m_J = \pm$ 15/2 ground state does not mix to any meaningful extent with excited states and is close to maximal axiality along z. Additionally, the energy of the phonon involved in the Raman process was kept fixed (see equation 2). The resulting fit is remarkably good given that only two parameters were fitted. Our analysis suggests that the $\{Dy_2(O_2)\}$ complex relaxes via spin-phonon coupling, whereas $\{Dy_2F_2\}$ relaxes too rapidly to allow for the investigation of the relaxation dynamics.

To gain further insights into the relaxation processes, we synthesised the Y diluted versions of the complexes. The dc measurements (Figures S11 and S12) show that the *ab initio* CF parameters are in good agreement with the experiments (max deviation 7% in $\{(Dy/Y)_2F_2\}$ **4** and 4% in $\{(Dy/Y)_2(O_2)\}$ **3**). $\{(Dy/Y)_2F_2\}$ **4** shows a shift to lower frequencies of the signals in the out of phase susceptibility measurements (Figure S13). The slow relaxation of $\{(Dy/Y)_2(O_2)\}$ **3** is profoundly different from the pure $\{Dy_2(O_2)\}$ isostructural complex (Figure 5). At zero applied field the relaxation time of the diluted complex is ca. 0.2 ms, one order of magnitude faster than that of the $\{Dy_2(O_2)\}$ complex and it does not significantly change over the whole investigated temperature range (Figure 5). This suggests that in the pure sample the Dy atoms exert an effective dc bias on their neighbour in the dimer, effectively quenching the QTM. When a dc field is applied to the diluted sample $\{(Dy/Y)_2(O_2)\}$, the χ'' curves show a double peak typical of multiple relaxation pathways[82] and there is no applied field able to provide the same qualitative picture of the $\{Dy_2(O_2)\}$ complex in zero field (see Figures S14–S16).

In order to compare the Raman relaxation of the diluted sample $\{(Dy/Y)_2(O_2)\}$ **3**, we also investigated the temperature dependence of the relaxation time at the same dc field (3000 Oe) applied on $\{Dy_2(O_2)\}$ **1**. The results of the fit, given in Table 1 and graphically in Figure 5 (green triangles), show that the energy of the resonant phonon is now ca. 23 cm^{-1}, slightly larger than the one found in the pure dimer, as expected from the smaller mass of the compound. If we change the applied field to the optimum field obtained from the field scan (H_{dc} = 1000 Oe, Figure S17), the fitting delivers virtually the same Raman term (both energy of the phonon and preexponential term) as in the case of the monomer (cyan stars in Figure 6). Therefore, in these complexes the Raman term appears to be

Table 1. Values obtained from the fit of the thermal evolution of the relaxation time of $\{Dy_2(O_2)\}$. Values in parenthesis are errors. Values without an error were fixed.

	$\{Dy_2(O_2)\}$	{Dy}	$\{Dy_2(O_2)\}$	$\{(Dy/Y)_2(O_2)\}$	$\{(Dy/Y)_2(O_2)\}$
H_{dc}	0 Oe	3000 Oe	3000 Oe	3000 Oe	1000 Oe
τ_{tun} [s]	2.0(1) 10^{-3}	–	–	–	–
B [s^{-1}]	$9.6(1.2)\cdot10^4$	$109(50)\cdot10^4$	$8.4(5.5)\cdot10^4$	$12(2)\cdot10^4$	$13(2)\cdot10^4$
$\hbar\omega$ [cm^{-1}]	16.5(6)	15.1(1.4)	16.5	22.9(7)	24.2(6)
D [s^{-1}]	–	–	10(1)	60(3)	1.7(2)
δ [cm^{-1}]	–	–	2.8	2.8	0.64

field-independent which is in contrast to the results of some recent theoretical and experimental studies.[35,37,83]

Conclusions

In summary, we report the successful coupling of a monomeric dysprosium complex to give dinuclear systems with the unusual linking units of a double fluoride bridge or side-on peroxide. Furthermore, this is a rare example of a lanthanide complex where a peroxo bridge was obtained through the deliberate addition of hydrogen peroxide.

The different nature of the bridging units leads to a shorter Dy–Dy distance in $\{Dy_2F_2\}$ than in $\{Dy_2(O_2)\}$ which leads to ferromagnetic dipolar coupling in $\{Dy_2F_2\}$, whereas in $\{Dy_2(O_2)\}$ the weaker dipolar interactions are likely compensated by an antiferromagnetic exchange contribution.

For the peroxido-bridged system slow relaxation was observed without the need to apply a dc field. Deletion of the second dysprosium by preparing a doped sample shows increased QTM. This reveals the importance of the second Dy ion providing a bias field to quench QTM.

For the three systems {Dy}, $\{Dy_2(O_2)\}$ and $\{(Dy/Y)_2(O_2)\}$ it was found that essentially the same Raman term governs the relaxation process. A central difference between the peroxido and the *bis*-fluorido bridged systems is the restriction of vibrational freedom in the former as a result of the rigidity of the O–O bond as recently highlighted by Tang *et al.*[65] This can affect both dipolar coupling directly, but also modify part of the phonon spectrum, which can be relevant. For both effects it seems intuitive that the more rigid system should be the better SMM.

Author Contributions

R.F.P. and J.Be.: Synthesis and development of synthetic strategies; M.B.: *ab initio* calculations; M.B. and M.P.: Theoretical analysis of magnetic data; N.B. and J.O.: Analysis of INS data; T.B.: Elemental analysis (metal and fluoride) by atomic absorption spectroscopy; S.P. and M.P.: SQUID measurements and evaluation; T.R., R.F.P., M.P., C.E.A. and J.Be.: Powder X-Ray diffractometry; C.E.A.: Crystallographic analysis; J.O., M.P. and R.F.P.: Collection of INS data; R.F.P., M.B., J.Br., C.E.A., M.P., J.Be. and A.K.P.: paper conceptualisation and writing as well as editing the manuscript. All authors contributed to reviewing and editing the manuscript and read and approved the submitted publication.

Acknowledgements

We thank the DFG CRC 1573 "4f for Future", the Helmholtz Gemeinschaft POF MSE and the Karlsruhe House of Young Scientists (KHYS) via the "Networking Grant" and the "Research Travel Grant" who made this collaboration between KIT, KU and UniFi possible. M.P. acknowledges funding from the European Research Council (ERC) under the European Union's Horizon 2020 research and innovation programme (Grant agreement No. 101039890). M.B. also thanks Fondazione Cassa di Risparmio di Firenze for the "Giovani Ricercatori Protagonisti" post-doctoral fellowship. Open Access funding enabled and organized by Projekt DEAL.

Conflict of Interests

The authors declare no conflict of interest.

Data Availability Statement

CCDC (https://www.ccdc.cam.ac.uk/structures/) Numbers: CCDC 2376535, 2376536 and 2376537

Keywords: Dysprosium · Axiality · Magnetic Relaxation · Magnetism · SMM

[1] N. Ishikawa, M. Sugita, T. Ishikawa, S.-Y. Koshihara, Y. Kaizu, *J. Am. Chem. Soc.* **2003**, *125*, 8694–8695.
[2] R. Sessoli, A. K. Powell, *Coord. Chem. Rev.* **2009**, *253*, 2328–2341.
[3] R. A. Layfield, M. Murugesu, *Lanthanides and Actinides in Molecular Magnetism*, Vol. 1, Wiley-VCH, Weinheim **2015**
[4] M. A. AlDamen, J. M. Clemente-Juan, E. Coronado, C. Marti-Gastaldo, A. Gaita-Arino, *J. Am. Chem. Soc.* **2008**, *130*, 8874–8875.
[5] S. D. Jiang, B. W. Wang, H. L. Sun, Z. M. Wang, S. Gao, *J. Am. Chem. Soc.* **2011**, *133*, 4730–4733.
[6] J. D. Rinehart, J. R. Long, *Chem. Sci.* **2011**, *2*, 2078–2085.
[7] L. Ungur, J. J. Le Roy, I. Korobkov, M. Murugesu, L. F. Chibotaru, *Angew. Chem. Int. Ed.* **2014**, *53*, 4413–4417.

[8] Y. C. Chen, J. L. Liu, L. Ungur, J. Liu, Q. W. Li, L. F. Wang, Z. P. Ni, L. F. Chibotaru, X. M. Chen, M. L. Tong, *J. Am. Chem. Soc.* **2016**, *138*, 2829–2837.
[9] Y. S. Ding, N. F. Chilton, R. E. Winpenny, Y. Z. Zheng, *Angew. Chem. Int. Ed.* **2016**, *55*, 16071–16074.
[10] C. A. P. Goodwin, F. Ortu, D. Reta, N. F. Chilton, D. P. Mills, *Nature* **2017**, *548*, 439–442.
[11] F.-S. Guo, B. M. Day, Y. C. Chen, M.-L. Tong, A. Mansikkamäki, R. A. Layfield, *Science* **2018**, *362*, 1400–1403.
[12] R. K. McClain, C. A. Gould, K. Chakarawet, S. J. Teat, T. J. Groshens, J. R. Long, B. G. Harvey, *Chem. Sci.* **2018**, *9*, 8492–8503.
[13] A. B. Canaj, S. Dey, E. R. Marti, C. Wilson, G. Rajaraman, M. Murrie, *Angew. Chem. Int. Ed.* **2019**, *58*, 14146–14151.
[14] A. B. Canaj, M. K. Singh, E. Regincos Marti, M. Damjanovic, C. Wilson, O. Cespedes, W. Wernsdorfer, G. Rajaraman, M. Murrie, *Chem. Commun.* **2019**, *55*, 5950–5953.
[15] M. Briganti, E. Lucaccini, L. Chelazzi, S. Ciattini, L. Sorace, R. Sessoli, F. Totti, M. Perfetti, *J. Am. Chem. Soc.* **2021**, *143*, 8108–8115.
[16] C. A. Gould, R. K. McClain, D. Reta, J. G. C. Kragskow, D. A. Marchiori, E. Lachman, E.-S. Choi, J. G. Analytis, R. D. Britt, N. F. Chilton, B. G. Harvey, J. R. Long, *Science* **2022**, *375*, 198–202.
[17] W. J. Xu, Q. C. Luo, Z. H. Li, Y. Q. Zhai, Y. Z. Zheng, *Adv. Sci.* **2024**, *11*, e2308548.
[18] K. L. M. Harriman, D. Errulat, M. Murugesu, *Trends Chem.* **2019**, *1*, 425–439.
[19] S. T. Liddle, J. van Slageren, *Chem. Soc. Rev.* **2015**, *44*, 6655–6669.
[20] A. Swain, T. Sharma, G. Rajaraman, *Chem. Commun.* **2023**, *59*, 3206–3228.
[21] V. S. Mironov, Y. G. Galyametdinov, A. Ceulemans, C. Görller-Walrand, K. Binnemans, *J. Chem. Phys.* **2002**, *116*, 4673–4685.
[22] L. Ungur, L. F. Chibotaru, *Inorg. Chem.* **2016**, *55*, 10043–10056.
[23] M. A. Sörensen, U. B. Hansen, M. Perfetti, K. S. Pedersen, E. Bartolome, G. G. Simeoni, H. Mutka, S. Rols, M. Jeong, I. Zivkovic, M. Retuerto, A. Arauzo, J. Bartolome, S. Piligkos, H. Weihe, L. H. Doerrer, J. van Slageren, H. M. Ronnow, K. Lefmann, J. Bendix, *Nat. Commun.* **2018**, *9*, 1292.
[24] N. A. Bonde, J. B. Petersen, M. A. Sorensen, U. G. Nielsen, B. Fak, S. Rols, J. Ollivier, H. Weihe, J. Bendix, M. Perfetti, *Inorg. Chem.* **2020**, *59*, 235–243.
[25] O. Cador, B. Le Guennic, L. Ouahab, F. Pointillart, *Eur. J. Inorg. Chem.* **2020**, *2020*, 148–164.
[26] T. T. Ruan, E. Moreno-Pineda, M. Schulze, S. Schlittenhardt, T. Brietzke, H. J. Holdt, S. K. Kuppusamy, W. Wernsdorfer, M. Ruben, *Inorg. Chem.* **2023**, *62*, 15148–15156.
[27] Y. Kishi, F. Pointillart, B. Lefeuvre, F. Riobe, B. Le Guennic, S. Golhen, O. Cador, O. Maury, H. Fujiwara, L. Ouahab, *Chem. Commun.* **2017**, *53*, 3575–3578.
[28] Y. S. Ding, K. X. Yu, D. Reta, F. Ortu, R. E. P. Winpenny, Y. Z. Zheng, N. F. Chilton, *Nat. Commun.* **2018**, *9*, 3134.
[29] C. A. P. Goodwin, F. Ortu, D. Reta, *Int. J. Quantum Chem.* **2020**, *120*(120), e26248.
[30] M. Li, H. Wu, Z. Xia, L. Ungur, D. Liu, L. F. Chibotaru, H. Ke, S. Chen, S. Gao, *Inorg. Chem.* **2020**, *59*, 7158–7166.
[31] L. Zhu, Y. Dong, B. Yin, P. Ma, D. Li, *Dalton Trans.* **2021**, *50*, 12607–12618.
[32] L. Scherthan, S. F. M. Schmidt, H. Auerbach, T. Hochdorffer, J. A. Wolny, W. Bi, J. Zhao, M. Y. Hu, T. Toellner, E. E. Alp, D. E. Brown, C. E. Anson, A. K. Powell, V. Schunemann, *Angew. Chem. Int. Ed.* **2019**, *58*, 3444–3449.
[33] L. Gu, R. Wu, *Phys. Rev. Lett.* **2020**, *125*, 117203.
[34] A. Lunghi, S. Sanvito, *J. Phys. Chem. Lett.* **2020**, *11*, 6273–6278.
[35] A. Lunghi, S. Sanvito, *J. Chem. Phys.* **2020**, *153*, 174113.
[36] L. Scherthan, R. F. Pfleger, H. Auerbach, T. Hochdörffer, J. A. Wolny, W. Bi, J. Zhao, M. Y. Hu, E. E. Alp, C. E. Anson, R. Diller, A. K. Powell, V. Schünemann, *Angew. Chem. Int. Ed.* **2020**, *59*, 8818–8822.
[37] M. Briganti, F. Santanni, L. Tesi, F. Totti, R. Sessoli, A. Lunghi, *J. Am. Chem. Soc.* **2021**, *143*, 13633–13645.
[38] L. Gu, R. Wu, *Phys. Rev. B* **2021**, *103*, 014401.
[39] F. Habib, P. H. Lin, J. Long, I. Korobkov, W. Wernsdorfer, M. Murugesu, *J. Am. Chem. Soc.* **2011**, *133*, 8830–8833.
[40] Y. Horii, K. Katoh, G. Cosquer, B. K. Breedlove, M. Yamashita, *Inorg. Chem.* **2016**, *55*, 11782–11790.
[41] P. Evans, D. Reta, C. A. P. Goodwin, F. Ortu, N. F. Chilton, D. P. Mills, *Chem. Commun.* **2020**, *56*, 5677–5680.
[42] T. Han, M. J. Giansiracusa, Z. H. Li, Y. S. Ding, N. F. Chilton, R. E. P. Winpenny, Y. Z. Zheng, *Chem. Eur. J.* **2020**, *26*, 6773–6777.
[43] R. F. Pfleger, S. Schlittenhardt, M. P. Merkel, M. Ruben, K. Fink, C. E. Anson, J. Bendix, A. K. Powell, *Chem. Eur. J.* **2021**, *27*, 15085–15094.
[44] P. B. Jin, Q. C. Luo, Y. Q. Zhai, Y. D. Wang, Y. Ma, L. Tian, X. Zhang, C. Ke, X. F. Zhang, Y. Lv, Y. Z. Zheng, *iScience* **2021**, *24*, 102760.
[45] P.-B. Jin, Q.-C. Luo, Y.-Y. Liu, Y.-Z. Zheng, *Sci. China Chem.* **2024**, *67*, 3328–3338.
[46] G. Brunet, F. Habib, I. Korobkov, M. Murugesu, *Inorg. Chem.* **2015**, *54*, 6195–6202.
[47] J. Dreiser, K. S. Pedersen, C. Piamonteze, S. Rusponi, Z. Salman, M. E. Ali, M. Schau-Magnussen, C. A. Thuesen, S. Piligkos, H. Weihe, H. Mutka, O. Waldmann, P. Oppeneer, J. Bendix, F. Nolting, H. Brune, *Chem. Sci.* **2012**, *3*, 1024–1032.
[48] Y. Huo, Y. C. Chen, S. G. Wu, J. L. Liu, J. H. Jia, W. B. Chen, B. L. Wang, Y. Q. Zhang, M. L. Tong, *Inorg. Chem.* **2019**, *58*, 1301–1308.
[49] S. K. Langley, C. M. Forsyth, B. Moubaraki, K. S. Murray, *Dalton Trans.* **2015**, *44*, 912–915.
[50] B. K. Ling, Y. Q. Zhai, J. Han, T. Han, Y. Z. Zheng, *Dalton Trans.* **2020**, *49*, 6969–6973.
[51] L. Norel, L. E. Darago, B. Le Guennic, K. Chakarawet, M. I. Gonzalez, J. H. Olshansky, S. Rigaut, J. R. Long, *Angew. Chem. Int. Ed.* **2018**, *57*, 1933–1938.
[52] K. S. Pedersen, M. A. Sørensen, J. Bendix, *Coord. Chem. Rev.* **2015**, *299*, 1–21.
[53] C. A. Thuesen, K. S. Pedersen, M. Schau-Magnussen, M. Evangelisti, J. Vibenholt, S. Piligkos, H. Weihe, J. Bendix, *Dalton Trans.* **2012**, *41*, 11284–11292.
[54] Q. Zhou, F. Yang, D. Liu, Y. Peng, G. Li, Z. Shi, S. Feng, *Inorg. Chem.* **2012**, *51*, 7529–7536.
[55] B.-K. Ling, Y.-Q. Zhai, P.-B. Jin, H.-F. Ding, X.-F. Zhang, Y. Lv, Z. Fu, J. Deng, M. Schulze, W. Wernsdorfer, Y.-Z. Zheng, *Matter* **2022**, *5*, 3485–3498.
[56] D. C. Bradley, J. S. Ghotra, F. A. Hart, M. B. Hursthouse, P. R. Raithby, *J. Chem. Soc. Dalton Trans.* **1977**, 1166–1172.
[57] G. B. Deacon, C. M. Forsyth, D. Freckmann, P. C. Junk, K. Konstas, J. Luu, G. Meyer, D. Werner, *Aust. J. Chem.* **2014**, *67*, 1860–1865.
[58] W. J. Gee, J. G. MacLellan, C. M. Forsyth, B. Moubaraki, K. S. Murray, P. C. Andrews, P. C. Junk, *Inorg. Chem.* **2012**, *51*, 8661–8663.
[59] V. Patroniak, M. Kubicki, A. Mondry, J. Lisowski, W. Radecka-Paryzek, *Dalton Trans.* **2004**, 3295–3304.
[60] M. Paul, S. Shirase, Y. Morimoto, L. Mathey, B. Murugesapandian, S. Tanaka, S. Itoh, H. Tsurugi, K. Mashima, *Chem. Eur. J.* **2016**, *22*, 4008–4014.
[61] N. P. Pook, A. Adam, *Z. Anorg. Allg. Chem.* **2014**, *640*, 2931–2938.
[62] D. M. Roitershtein, A. A. Vinogradov, K. A. Lyssenko, I. E. Nifant'ev, *Inorg. Chem. Commun.* **2017**, *84*, 225–228.
[63] Y.-L. Sang, X.-S. Lin, X.-C. Li, Y.-H. Liu, X.-H. Zhang, *Inorg. Chem. Commun.* **2015**, *62*, 115–118.
[64] G. C. Wang, Y. M. So, K. L. Wong, K. C. Au-Yeung, H. H. Sung, I. D. Williams, W. H. Leung, *Chem. Eur. J.* **2015**, *21*, 16126–16135.
[65] G. C. Wang, H. H. Sung, I. D. Williams, W. H. Leung, *Inorg. Chem.* **2012**, *51*, 3640–3647.
[66] Y. Zhang, J. Wu, S. Shen, Z. Liu, J. Tang, *Polyhedron* **2018**, *150*, 40–46.
[67] X. Liu, C. Zhao, J. Wu, Z. Zhu, J. Tang, *Dalton Trans.* **2022**, *51*, 16444–16447.
[68] C. Zhao, T. Wang, X. Liu, Z. Zhu, X. Ying, X. L. Li, J. Tang, *Dalton Trans.* **2023**, *52*, 15456–15461.
[69] J. D. Curry, M. A. Robinson, D. H. Busch, *Inorg. Chem.* **1967**, *6*, 1570–1574.
[70] Z. X. Jiang, J. L. Liu, Y. C. Chen, J. Liu, J. H. Jia, M. L. Tong, *Chem. Commun.* **2016**, *52*, 6261–6264.
[71] M. Sakamoto, N. Matsumoto, H. Okawa, *Bull. Chem. Soc. Jpn.* **1991**, *64*, 691–693.
[72] F. S. Keij, R. A. G. de Graaff, J. G. Haasnoot, A. J. Oosterling, E. Perdersen, J. Reedijk, *J. Chem. Soc., Chem. Commun.* **1988**, 423–425.
[73] M. Ghiladi, C. J. McKenzie, A. Meier, A. K. Powell, J. Ulstrup, S. Wocadlo, *Dalton Trans.* **1997**, 4011–4018.
[74] L. F. Chibotaru, L. Ungur, *J. Chem. Phys.* **2012**, *137*, 064112.
[75] L. Ungur, L. F. Chibotaru, *Chem. Eur. J.* **2017**, *23*, 3708–3718.
[76] N. F. Chilton, D. Collison, E. J. McInnes, R. E. Winpenny, A. Soncini, *Nat. Commun.* **2013**, *4*, 2551.
[77] K. D. Karlin, Z. Tyeklar, A. Farooq, R. R. Jacobson, *Inorg. Chim. Acta* **1991**, *182*, 1–3.
[78] L. E. Roy, T. Hughbanks, *J. Am. Chem. Soc.* **2005**, *128*, 568–575.

[79] P. Kumar, J. Flores Gonzalez, P. P. Sahu, N. Ahmed, J. Acharya, V. Kumar, O. Cador, F. Pointillart, S. K. Singh, V. Chandrasekhar, *Inorg. Chem. Front.* **2022**, *9*, 5072–5092.
[80] Y. Huo, Y.-C. Chen, S.-G. Wu, J.-L. Liu, J.-H. Jia, W.-B. Chen, B.-L. Wang, Y.-Q. Zhang, M.-L. Tong, *Inorg. Chem.* **2019**, *58*, 1301–1308.
[81] Q. Zhou, F. Yang, D. Liu, Y. Peng, G. Li, Z. Shi, S. Feng, *Inorg. Chem.* **2012**, *51*, 7529–7536.
[82] P.-E. Car, M. Perfetti, M. Mannini, A. Favre, A. Caneschi, R. Sessoli, *Chem. Commun.* **2011**, *47*, 3751–3753.
[83] F. S. Santana, M. Perfetti, M. Briganti, F. Sacco, G. Poneti, E. Ravera, J. F. Soares, R. Sessoli, *Chem. Sci.* **2022**, *13*, 5860–5871.

Manuscript received: August 9, 2024
Accepted manuscript online: October 7, 2024
Version of record online: November 16, 2024